Available online at www.sciencedirect.com
SCIENCE DIRECT®
Journal of Fluorine Chemistry 124 (2003) 189–196
JOURNAL OF FLUORINE CHEMISTRY
www.elsevier.com/locate/jfluchem

Synthesis and solution properties of sulfate-type hybrid surfactants with a benzene ring

Haruhiko Miyazawa[a], Kanako Igawa[a], Yukishige Kondo[a,b], Norio Yoshino[a,b,*]

[a]*Department of Industrial Chemistry, Faculty of Engineering, Tokyo University of Science, 1-3 Kagurazaka, Shinjuku-ku, Tokyo 162-8601, Japan*
[b]*Institute of Colloid and Interface Science, Tokyo University of Science, 1-3 Kagurazaka, Shinjuku-ku, Tokyo 162-8601, Japan*

Received 21 April 2003; received in revised form 13 August 2003; accepted 14 August 2003

Abstract

Nine novel sulfate-type hybrid surfactants, $C_mF_{2m+1}C_6H_4CH(OSO_3Na)C_nH_{2n+1}$ (F*m*PH*n*OS: $m = 4, 6, 8$; $n = 3, 5, 7$; C_6H_4: *p*-phenylene), with a benzene ring in their molecules were synthesized. Alkanoyl chlorides were allowed to react with iodobenzene in the presence of aluminum chloride to give the corresponding aromatic ketones. The reaction of the ketones with perfluoroalkyl iodides yielded 1-[4-(perfluoroalkyl)phenyl]-1-alkanones as intermediates. The intermediates were allowed to react with methanol in tetrahydrofuran in the presence of sodium borohydride to yield 1-[4-(perfluoroalkyl)phenyl]-1-alkanols. The desired hybrid surfactants were obtained by the reaction of 1-[4-(perfluoroalkyl)phenyl-1-alkanols with sulfur trioxide/pyridine complex in pyridine and by the subsequent neutralization of the products with sodium hydroxide solution. When compared with the conventional hybrid surfactants, $C_mF_{2m+1}C_6H_4COCH(SO_3Na)C_nH_{2n+1}$ (F*m*H*n*S: $m = 4, 6$; $n = 2, 4, 6$; C_6H_4: *p*-phenylene), the new hybrid surfactants thus synthesized were found to have a comparable ability to lower the surface tension of water and a high hydrophilicity. The cmc of F*m*PH*n*OS obeyed Kleven's rule and their occupied areas per molecule increased with increasing *m* and *n* with the values between 0.66 and 1.05 nm^2. The aggregation number for F*m*PH*n*OS micelles ranged from 6 to 45 and the hydrodynamic radius of the micelles was in the range of 1.4–3.1 nm.

Keywords: Hybrid surfactant; Benzene ring; Sulfate; Critical micelle concentration; Surface tension at cmc; Krafft point; Occupied area per molecule; Aggregation number; Hydrodynamic radius

1. Introduction

Fluorinated surfactants with a fluorocarbon chain as the hydrophobic group exhibit characteristic properties including thermal resistance, chemical resistance, high surface activity, high surface modifying ability and low critical micelle concentration [1–4]. Although mixing with fluorinated surfactants was attempted to give their characteristic properties to hydrocarbon surfactants, the attempt failed because no well-mixed surfactant micelle was formed while fluorinated surfactant-rich and hydrocarbon surfactant-rich micelles were found to form in the mixture [5–10]. Guo et al. synthesized hybrid surfactants with a fluorocarbon chain and a hydrocarbon chain in one molecule, $C_mF_{2m+1}CH(OSO_3Na)C_nH_{2n+1}$ (F*m*H*n*: $m = 6, 7, 8, 9$; $n = 1, 2, 3, 4, 5, 6, 7, 8, 9$), in 1992 [11]. However, these surfactants were easily hydrolyzed by moisture in the air, making them practically useless. The present authors synthesized six sulfonate-type hybrid surfactants with a benzene ring in their molecule, $C_mF_{2m+1}C_6H_4COCH_2(SO_3Na)C_nH_{2n+1}$ (F*m*H*n*S: $m = 4, 6$; $n = 2, 4, 6$; C_6H_4: *p*-phenylene), in 1995 [12], and have reported that the surfactants are hardly hydrolyzable and are thermoresistant up to 200 °C, and have an excellent surface tension lowering ability, and 10 wt.% F6H4S aqueous solution exhibits a very high visco elasticity at 37 °C [13–16]. Because of low interfacial tension, F*m*H*n*S could emulsify mutually immiscible ternary system, hydrocarbon/water/perfluoropolyether, simultaneously [12,17]. In addition, intramicellar phase separation has been observed to occur between fluorocarbon chains and hydrocarbon chains in aqueous solution of F*m*H*n*S [18].

The present paper reports the synthesis of nine novel sulfate-type hybrid surfactants, $C_mF_{2m+1}C_6H_4CH(OSO_3Na)C_nH_{2n+1}$ (F*m*PH*n*OS: $m = 4, 6, 8$; $n = 3, 5, 7$; C_6H_4:

* Corresponding author. Tel.: +81-3-5228-8319; fax: +81-3-3260-4281.
E-mail address: yoshino@ci.kagu.tus.ac.jp (N. Yoshino).

0022-1139/$ – see front matter © 2003 Published by Elsevier B.V.
doi:10.1016/j.jfluchem.2003.08.007

p-phenylene) and the physicochemical properties of their solutions.

2. Result and discussion

2.1. Synthesis of hybrid surfactants

Scheme 1 is the route of synthesis of the hybrid surfactants.

All reactions proceeded in mild conditions. The yield of F*m*PH*n*A was higher than 80%. An attempt failed to sulfate F*m*PH*n*A with concentrated sulfuric acid and fuming sulfuric acid to obtain F*m*PH*n*OS. However, SO_3/pyridine complex with a lower SO_3 activity was found to give F*m*PH*n*OS in a high yield. Only 2.0 mg of water was absorbed when F6PH5OS (104.0 mg) was exposed to the air for 10 days. After F6PH5OS with absorbed water was dried for 3 h under reduced pressure 20 Pa, ^{1}H NMR and FT-IR spectra of the dried surfactant were measured. The spectra obtained were the same as those of pure F6PH5OS. F*m*H*n* [11] are easily hydrolyzed since a strongly electron attracting fluorocarbon group and a sulfate ester group bind to the same carbon atom in their molecules, whereas the hybrid surfactants synthesized in the present work are hardly susceptible to hydrolysis because of the presence of a benzene ring between the fluorocarbon and sulfate ester groups in their molecules.

2.2. Krafft point, cmc, and surface tension of FmPHnOS

Table 1 lists the cmc, surface tension at cmc (γ_{cmc}), and Krafft point (K_p) for F*m*PH*n*OS.

The cmc was determined using surface tension and ^{1}H NMR measurements. No big difference was found between the cmc determined by two methods. The γ_{cmc} for F*m*PH*n*OS was around 20 mN/m which was almost same as that for F*m*H*n*S [19] or the conventional single-chain fluorinated surfactant [20]. The hydrophilicity of F*m*PH*n*OS was slightly higher than that of F*m*H*n*S [19]. Fig. 1 shows the relationship between surface tension and concentration for F*m*PH*n*OS aqueous solution.

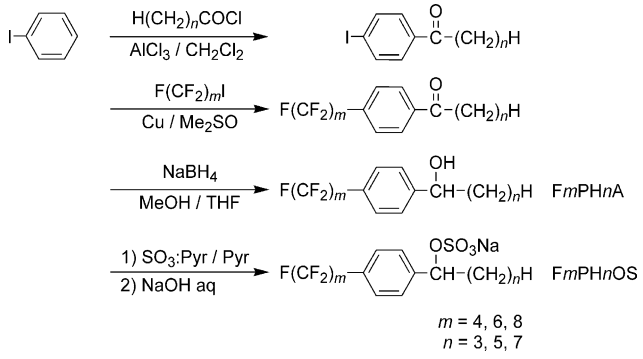

Scheme 1. Synthesis of F*m*PH*n*OS.

Table 1
Cmc, surface tension at cmc (γ_{cmc}), and Krafft point (K_p) for F*m*PH*n*OS

Surfactant	cmc		γ_{cmc} (mN/m)	K_p[c] (°C)
	Surface tension[a] (mM)	^{1}H NMR[b] (mM)		
F4PH3OS	7.0	7.0	19	<0 (35 mM)
F6PH3OS	0.90	0.81	18	<0 (4.5 mM)
F8PH3OS	0.08	–[d]	20	16 (0.4 mM)
F4PH5OS	3.0	3.6	19	<0 (10 mM)
F6PH5OS	0.34	0.30	20	14 (1.5 mM)
F8PH5OS[e]	–	–	–	32 (0.2 mM)
F4PH7OS	1.3	1.3	20	8 (6.5 mM)
F6PH7OS[e]	–	–	–	43 (0.5 mM)
F8PH7OS[e]	–	–	–	76(0.01 mM)

[a] 27 °C.
[b] 30 °C.
[c] K_p was measured in the concentration shown in parenthesis.
[d] Accurate cmc of FBPH3OS was not obtained because of low ^{1}H NMR signal intensities.
[e] These data except for K_p were not obtained because of high K_p.

The occupied area per molecule for F*m*PH*n*OS was calculated from the surface excess concentration at air/water interface (Γ). Γ was calculated using the Gibbs adsorption isotherm (1) [20].

$$\Gamma = -\frac{1}{4.606RT}\left(\frac{\partial\gamma}{\partial \log C}\right) \quad (1)$$

Here, R is the gas constant and T is the absolute temperature. The occupied area (A) per molecule for F*m*PH*n*OS relates to the adsorption amount Γ via the following Eq. (2).

$$A = \frac{1}{\Gamma N_A} \quad (2)$$

where N_A is Avogadro's number.

Table 2 shows the surface excess concentration Γ and A for F*m*PH*n*OS.

The value A increased with increasing m and n. The value of A was 0.66–1.04 nm^2/molecule, while for sodium alkyl

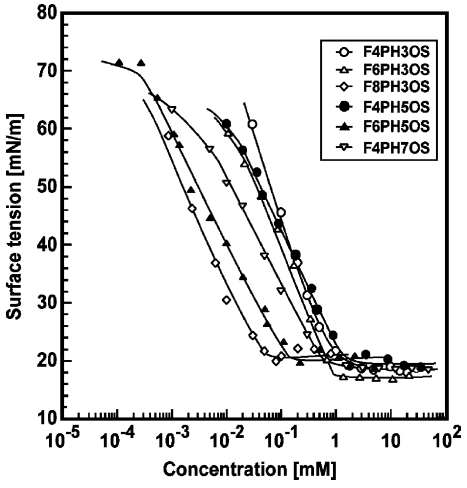

Fig. 1. Surface tension plots of F*m*PH*n*OS against concentration at 27 °C.

Table 2
Surface excess concentration Γ and occupied area A per molecular at 27 °C

Surfactant	Γ (μmol/m^2)	A (nm^2)
F4PH3OS	2.5	0.66
F6PH3OS	2.1	0.80
F8PH3OS	1.8	0.94
F4PH5OS	1.7	0.99
F6PH5OS	1.6	1.04
F4PH7OS	1.6	1.04

sulfates having two alkyl chains such as $(C_{10}H_{21})(C_7H_{15})$-$CHOSO_3Na$ it was 0.50–0.60 nm^2/molecule [20]. The values A for FmPHnOS were smaller than those for FmHnS (0.81 and 1.06 nm^2 for F4H2S and F4H6S, respectively [19]) when the lengths of hydrocarbon chain n and fluorocarbon chain m are respectively about the same for both types of hybrid surfactants. The A value depends on the species of hydrophilic group rather than those of hydrophobic group [20]. Since FmHnS has a hydrophilic carbonyl group that can form hydrogen bond with water molecule, this surfactant has two hydrophilic groups. This would make the value A of the surfactant larger than that of FmPHnOS. Fig. 2 shows the logarithmic plots of the cmc determined by surface tension measurement against m and n.

In the case of FmPH3OS, log(cmc) decreased linearly with increasing m, obeying Kleven's rule (3).

$$\log(\text{cmc}) = -0.186 - 0.486m \quad (\text{correlation coefficient}, 0.998) \quad (3)$$

This rule also holds for F4PHnOS with respect to n, Eq. (4).

$$\log(\text{cmc}) = -1.61 - 0.183n \quad (\text{correlation coefficient}, 0.999) \quad (4)$$

Eqs. (3) and (4) suggest that when the number of CH_2 or CF_2 group in the hydrophobic chain increases by one, the cmc decreases by 34 or 67%, respectively.

If Kleven's rule is assumed to hold for FmPH5OS ($n = 5$) and F6PHnOS ($m = 6$), even though only two cmc are available for the surfactants, the following two Eqs. (5) and (6) are obtained.

$$\text{F}m\text{PH5OS}: \quad \log(\text{cmc}) = -0.633 - 0.473m \quad (5)$$

$$\text{F6PH}n\text{OS}: \quad \log(\text{cmc}) = -2.41 - 0.211n \quad (6)$$

These equations give the rates of cmc decrease of 38% per CH_2 group and 66% per CF_2 group for F6PHnOS and FmPH5OS, respectively. With FmHn, cmc decreases by 35 and 75% when the number of CH_2 group and CF_2 group, respectively, increase by one [11]. A comparison of the contribution to cmc of CH_2 group or CF_2 group between FmPHnOS and FmHn reveals that the contribution of CF_2 group is smaller for FmPHnOS than for FmHn while that of CH_2 group is almost the same for both types of surfactants. The smaller contribution of CF_2 group for FmPHnOS would be brought about by the introduction of a spatially large benzene ring between the fluorocarbon chain and the hydrophilic group, thereby causing weakened hydrophobic interaction between fluorocarbon chains as compared with that for FmHn.

2.3. Aggregation number and diameter of FmPHnOS micelles

Fig. 3 shows the relationship between the ^{1}H NMR chemical shift δ_{obs} for ω-CH_3 group and the reciprocal concentration for F4PH3OS.

The δ_{obs} at concentrations lower than cmc are for the chemical shift for monomer δ_{mon} while those at concentrations higher than cmc are the weight average of the chemical shift for monomer and that for micelle δ_{mic} [21]. The following relation (7) then holds among δ_{obs}, δ_{mon}, and δ_{mic}:

$$\delta_{obs} = p_{mon}\delta_{mon} + (1 - p_{mon})\delta_{mic} \quad (7)$$

$$p_{mon} = \frac{C_{mon}}{C} \quad (8)$$

where C_{mon} and p_{mon} are the concentration and mole fraction of monomer. Since changes in the monomer concentration

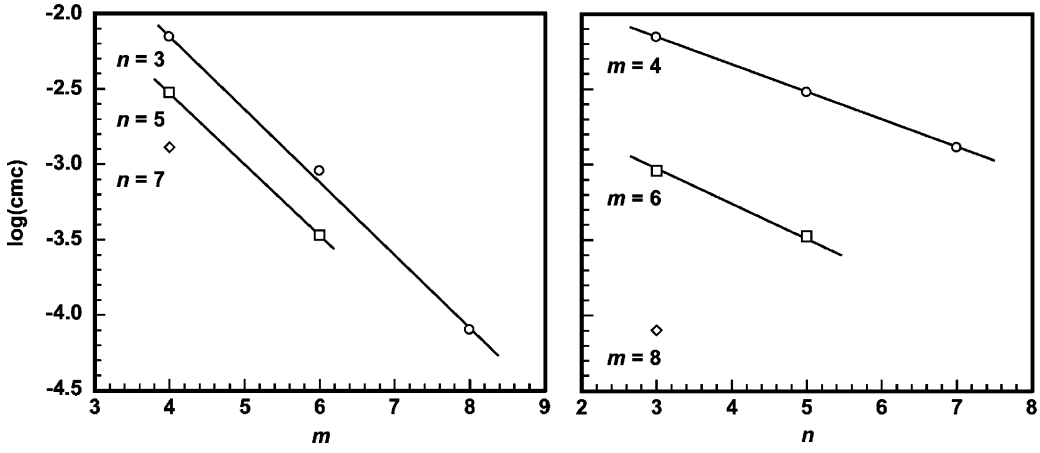

Fig. 2. Plots of log(cmc) for FmPHnOS against m and n.

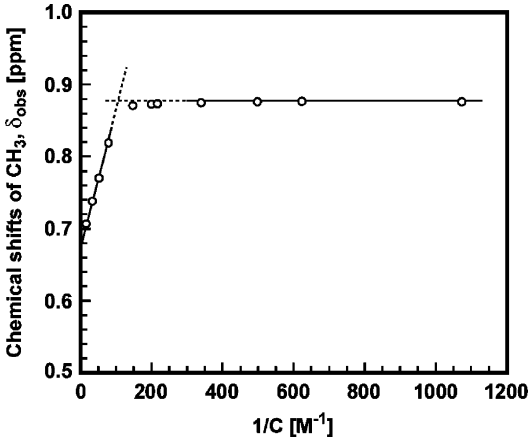

Fig. 3. Chemical shift plot for ω-CH_3 group in F4PH3OS against reciprocal concentration.

can be neglected above cmc, δ_{obs} is linearly related with $1/C$ as in (9).

$$\delta_{obs} = \delta_{mic} + \frac{(\delta_{mon} - \delta_{mic})\text{cmc}}{C} \quad (9)$$

The concentration at the intersection of the two lines in Fig. 3 gives cmc [11], and the δ_{obs} at $1/C \rightarrow 0$ corresponding to δ_{mic}.

On the other hand, the mass action model for micelle formation is given by Eq. (10), assuming no effect from the counterion and also assuming one single micelle size with a well-defined aggregation number [22,23]:

$$N\,\mathrm{S} \leftrightarrows \mathrm{S}_N \quad (10)$$

where N is the aggregation number and S and S_N denote respectively monomer and micelle. The equilibrium constant K for micelle formation according to Eq. (10) can be written in the form (11):

$$K = \frac{[\mathrm{S}_N]}{[\mathrm{S}]^N} \quad (11)$$

$$[\mathrm{S}] = C_{mon} \quad (12)$$

$$[\mathrm{S}_N] = \frac{C_{mic}}{N} \quad (13)$$

where C_{mic} is the concentration of F*m*PH*n*OS forming micelles. Substituting Eqs. (12) and (13) into Eq. (11) and taking the logarithms of both sides the resulting equation yield Eq. (14).

$$\log C_{mic} - N \log C_{mon} = \log NK = \text{constant} \quad (14)$$

Then, the plot of log C_{mic} against log C_{mon} gives a straight line, the slope of which allows to determine the aggregation number N. C_{mon} and C_{mic} can be calculated using the following equations with the δ_{obs}.

$$C_{mon} = p_{mon}C = \frac{\delta_{obs} - \delta_{mic}}{\delta_{mon} - \delta_{mic}} C \quad (15)$$

$$C_{mic} = (1 - p_{mon})C = \frac{\delta_{mon} - \delta_{obs}}{\delta_{mon} - \delta_{mic}} C \quad (16)$$

Table 3
Diffusion coefficient of the surfactants (D_{obs}), micelle (D_{mic}), monomer (D_{mon}), and hydrodynamic radius (R_H) for F*m*PH*n*OS in D_2O at 30 °C

Surfactant	N	D_{obs} ($10\ nm^2/s$)	D_{mic} ($10\ nm^2/s$)	D_{mon} ($10\ nm^2/s$)	R_H (nm)
F4PH3OS	6	0.32	0.17	0.75	1.4
F6PH3OS	–	0.22	0.095	0.57	1.8
F4PH5OS	15	0.21	0.10	0.65	2.2
F6PH5OS[a]	–	0.21	0.17	0.39	1.1
F4PH7OS	45	0.38	0.074	0.54	3.1

[a] Data from [21].

Table 3 shows the aggregation numbers N for F*m*PH*n*OS. The numbers for F6PH3OS and F6PH5OS could not be determined because the hydrodynamic radius of their micelles changed at concentrations above the cmc [21]. The value N was found to increase exponentially with increasing length of hydrocarbon chain n.

The diffusion coefficient of F*m*PH*n*OS micelles was determined by the pulsed-gradient spin echo (PGSE) method. The diffusion coefficient D_{obs} for F*m*PH*n*OS at concentrations higher than cmc is the weight average of those for monomer D_{mon} and micelle D_{mic} as is given by Eq. (17) [21].

$$D_{obs} = p_{mon}D_{mon} + (1 - p_{mon})D_{mic} \quad (17)$$

If the monomer concentration is assumed to be constant at concentrations above cmc, that is, $C_{mon} \approx$ cmc, then Eq. (17) is written simply as:

$$D_{obs} = \frac{\text{cmc}}{C} D_{mon} + \left(\frac{C - \text{cmc}}{C}\right) D_{mic} \quad (18)$$

Thus, D_{mic} can be obtained from the D_{obs} measured at concentrations below cmc, which is equal to D_{mon}.

Table 3 shows the values of D_{obs}, D_{mic} and D_{mon} at a concentration four times higher than cmc, and hydrodynamic radius of micelle R_H. The hydrodynamic micelle radius was calculated using the Stokes–Einstein equation:

$$R_H = \frac{kT}{6\pi\eta_0 D} \quad (19)$$

where k is the Boltzmann constant and η_0 is the viscosity of solvent. The hydrodynamic radius of F6PH5OS micelle was smaller than that of F4PH3OS micelle, though the radius of surfactant micelle generally increases with increasing length of the hydrophobic chain. This would presumably be due to an interdigitated structure of F6PH5OS micelle [21].

3. Conclusion

Novel sulfate-type hybrid surfactants, $C_mF_{2m+1}C_6H_4CH(OSO_3Na)C_nH_{2n+1}$ (F*m*PH*n*OS: $m = 4, 6, 8$; $n = 3, 5, 7$), were synthesized in a relatively high yield. These surfactants were stable and hardly hydrolyzed and had surface activity as high as that of the conventional surfactants, while they showed a lower Krafft point.

The cmc for F*m*PH*n*OS obeyed Kleven's rule and the decreasing rates of their cmc with increasing hydrophobic chain length were 34–38% per CH_2 group and 66–67% per CF_2 group, respectively. The occupied area per molecule for F*m*PH*n*OS increased with increasing length of fluorocarbon chain or hydrocarbon chain, and the area ranged from 0.66 to 1.04 nm^2.

The aggregation number of F*m*PH*n*OS molecules forming a micelle increased abruptly with increasing *n* and the hydrodynamic radius of F*m*PH*n*OS micelle was in a range 1.4–3.1 nm.

4. Experimental

4.1. Materials

$IC_6H_4COC_nH_{2n+1}$ ($n = 3$, 5, 7) and $C_mF_{2m+1}C_6H_4$-COC_nH_{2n+1} ($m = 4$, 6, 8; $n = 3$, 5, 7) were synthesized as reported previously [12]. Sulfur trioxide/pyridine complex, sodium hydroxide (all from Kanto Kagaku), and sodium borohydride (Nacalai Tesque) were used as supplied. Tetrahydrofuran (THF: bp 65 °C) used as a solvent was purified by distillation after being dehydrated with calcium hydride. The other commercially available solvents (diethyl ether, hexane, methanol, and pyridine) were used without further purification.

4.2. Measurements and instruments

A Nicolet Avatar 360-FT-IR spectrometer was used to measure FT-IR spectrum with the ATR method. A Bruker DPX-400 spectrometer was used to measure 400 MHz ^1H NMR spectrum at 30 °C in $CDCl_3$, CD_3OD (with tetramethylsilane (TMS) as the internal standard), or D_2O. The same spectrometer was also used to measure 376 MHz ^{19}F NMR spectrum at 30 °C in $CDCl_3$ or CD_3OD (with trifluoroacetic acid as external standard). GC–mass spectrum (GC–MS) was measured with a Hewlett-Packard HP6890 series GC System (Hewlett-Packard 5973 Mass Selective Detector). MS measurement (FABMS) using the Fast Atom Bombardment (FAB) method was performed with a JEOL JMS SX102A. Surface tension was measured at 27 °C by the Wilhelmy method using a Krüss Model K12 surface tensiometer. Electroconductivity measurement was conducted on surfactant solution as a function of temperature with a DKK-TOA conductivity meter CM-60S and the temperature at which the conductivity abruptly changes was defined as the Krafft point of the surfactant. The cmc and the aggregation number of F*m*PH*n*OS were determined for their D_2O solution by plotting the ^1H NMR chemical shift of ω-CH_3 against the reciprocal concentration according to the method previously reported [11]. The diffusion coefficient of F*m*PH*n*OS was measured on the ^1H NMR chemical shift for ω-CH_3 by the pulsed-gradient spin echo (PGSE) method [24]. The gradient intensity was calibrated before measurement using the diffusion coefficient of H_2O ($D_{obs} = 2.3 \times 10^{-9}$ m^2/s [25]).

4.3. Synthesis of hybrid alcohols

4.3.1. Synthesis of 1-[4-(perfluorobutyl)phenyl]-1-butanol (F4PH3A)

$C_4F_9C_6H_4COC_3H_7$ (22.3 g, 60.8 mmol) [12], sodium borohydride (0.689 g, 18.2 mmol), and THF (50 cm^3) were placed in a 300 ml eggplant-shaped flask equipped with an isobaric dropping funnel, through which methanol (30.1 g, 939 mmol) was then slowly added dropwise under ice-cooling. After the reaction mixture was stirred for 5 h at room temperature, THF and methanol were removed by distillation under reduced pressure. The ether-soluble part of the residue was washed with water and dehydrated with magnesium sulfate. Removal of diethyl ether by distillation under reduced pressure from this part gave F4PH3A as a colorless transparent viscous liquid. IR (cm^{-1}): 3130–3337 (ν_{O-H}), 2880–2957 (ν_{C-H}), 1243 (ν_{C-F}); ^1H NMR ($CDCl_3$): δ 0.93 (3H, t, $J = 7.3$ Hz, *a*), 1.27 (2H, m, *b*), 1.58 (2H, dd, *c*), 4.61 (1H, t, $J = 7.1$ Hz, *d*), 2.34 (1H, s, *e*), 7.36 (2H, d, $J = 8.2$ Hz, *m*-protons from C_4F_9), 7.46 (2H, d, $J = 8.2$ Hz, *o*-protons from C_4F_9) for $CH_3{}^aCH_2{}^bCH_2{}^cCH^d(OH)^eC_6H_4$-$C_4F_9$; ^{19}F NMR ($CDCl_3$): δ −81.3 (3F, s, *a*), −126.6 (2F, s, *b*), −122.3 (2F, s, *c*), −111.4 (2F, s, *d*) for $CF_3{}^aCF_2{}^bCF_2{}^cCF_2{}^dC_6H_4CH(OH)C_3H_7$; GC–MS 70 eV, *m/z* (rel. int.): 368 $[M]^+$ (1.2), 325 $[M–C_3H_7]^+$ (100), 277 $[C_4F_8C_6H_5]^+$ (33), 156 $[CF_2C_6H_4CH(OH)]^+$ (15), 127 $[CF_2C_6H_5]^+$ (25).

4.3.2. Synthesis of 1-[4-(perfluorohexyl)phenyl]-1-butanol (F6PH3A), etc.

The methods of synthesis and purification were the same as those used in Section 4.3.1.

F6PH3A: white solid; IR (cm^{-1}): 3149–3350 (ν_{O-H}), 2844–2963 (ν_{C-H}), 1240 (ν_{C-F}); ^1H NMR ($CDCl_3$): δ 0.96 (3H, t, $J = 7.4$ Hz, *a*), 1.36 (2H, m, *b*), 1.74 (2H, dd, *c*), 4.78 (1H, t, $J = 5.2$ Hz, *d*), 1.91 (1H, s, *e*), 7.49 (2H, d, $J = 8.2$ Hz, *m*-protons from C_6F_{13}), 7.58 (2H, d, $J = 8.2$ Hz, *o*-protons from C_6F_{13}) for $CH_3{}^aCH_2{}^bCH_2{}^cCH^d$-$(OH)^eC_6H_4C_6F_{13}$; ^{19}F NMR ($CDCl_3$): δ −81.5 (3F, s, *a*), −126.2 (2F, s, *b*), −123.4 (2F, s, *c*), −122.3 (2F, s, *d*), −122.0 (2F, s, *e*), −111.3 (2F, s, *f*) for $CF_3{}^aCF_2{}^bCF_2{}^cCF_2{}^dCF_2{}^e$-$CF_2{}^fC_6H_4CH(OH)C_3H_7$; GC–MS 70 eV, *m/z* (rel. int.): 468 $[M]^+$ (1.4), 425 $[M–C_3H_7]^+$ (100), 377 $[C_6F_{12}C_6H_5]^+$ (43), 156 $[CF_2C_6H_4CH(OH)]^+$ (32), 127 $[CF_2C_6H_5]^+$ (41).

F8PH3A: white solid; IR (cm^{-1}): 3131–3550 (ν_{O-H}), 2810–2998 (ν_{C-H}), 1233 (ν_{C-F}); ^1H NMR ($CDCl_3$): δ 0.96 (3H, t, $J = 7.4$ Hz, *a*), 1.36 (2H, m, *b*), 1.74 (2H, dd, *c*), 4.78 (1H, t, $J = 5.2$ Hz, *d*), 1.91 (1H, s, *e*), 7.49 (2H, d, $J = 8.2$ Hz, *m*-protons from C_8F_{17}), 7.58 (2H, d, $J = 8.2$ Hz, *o*-protons from C_8F_{17}) for $CH_3{}^aCH_2{}^bCH_2{}^cCH_2{}^d$-$(OH)^eC_6H_4C_8F_{17}$; ^{19}F NMR ($CDCl_3$): δ −81.3 (3F, s, *a*),

−126.6 (2F, s, *b*), −123.3 (2F, s, *c*), −122.3 (6F, s, *d*, *e* and *f*), −121.7 (2F, s, *g*), −111.0 (2F, s, *h*) for $CF_3{}^aCF_2{}^bCF_2{}^cCF_2{}^d$-$CF_2{}^eCF_2{}^fCF_2{}^gCF_2{}^hC_6H_4CH(OH)C_3H_7$; GC–MS 70 eV, *m/z* (rel. int.): 468 $[M]^+$ (1.4), 425 $[M–C_3H_7]^+$ (100), 377 $[C_6F_{12}C_6H_5]^+$ (43), 156 $[CF_2C_6H_4CH(OH)]^+$ (32), 127 $[CF_2C_6H_5]^+$ (41).

F4PH5A: colorless liquid; IR (cm^{-1}): 3165–3343 ($\nu_{O–H}$), 2845–2961 ($\nu_{C–H}$), 1236 ($\nu_{C–F}$); ^1H NMR ($CDCl_3$): δ 0.88 (3H, t, $J = 7.3$ Hz, *a*), 1.31 (6H, m, *b*, *c* and *d*), 1.72 (2H, m, *e*), 4.72 (1H, t, $J = 5.8$ Hz, *f*), 1.92 (1H, s, *g*), 7.47 (2H, d, $J = 8.1$ Hz, *m*-protons from C_4F_9), 7.54 (2H, d, $J = 8.2$ Hz, *o*-protons from C_4F_9) for $CH_3{}^aCH_2{}^bCH_2{}^cCH_2{}^dCH_2{}^eCH^f$-$(OH)^gC_6H_4C_4F_9$; ^{19}F NMR ($CDCl_3$): δ −81.3 (3F, s, *a*), −126.6 (2F, s, *b*), −122.3 (2F, s, *c*), −111.2 (2F, s, *d*) for $CF_3{}^aCF_2{}^bCF_2{}^cCF_2{}^dC_6H_4CH(OH)C_5H_{11}$; GC–MS 70 eV, *m/z* (rel. int.): 396 $[M]^+$ (1.3), 325 $[M–C_5H_{11}]^+$ (100), 277 $[C_4F_8C_6H_5]^+$ (34), 156 $[CF_2C_6H_4CH(OH)]^+$ (14), 127 $[CF_2C_6H_5]^+$ (25).

F6PH5A: colorless liquid; IR (cm^{-1}): 3153–3340 ($\nu_{O–H}$), 2847–2960 ($\nu_{C–H}$), 1240 ($\nu_{C–F}$); ^1H NMR ($CDCl_3$): δ 0.89 (3H, t, $J = 7.2$ Hz, *a*), 1.30 (6H, m, *b*, *c* and *d*), 1.72 (2H, m, *e*), 4.74 (1H, t, $J = 5.7$ Hz, *f*), 1.93 (1H, s, *g*), 7.48 (2H, d, $J = 8.1$ Hz, *m*-protons from C_6F_{13}), 7.56 (2H, d, $J = 8.2$ Hz, *o*-protons from C_6F_{13}) for $CH_3{}^aCH_2{}^bCH_2{}^cCH_2$-$^dCH_2{}^eCH^f(OH)^gC_6H_4C_6F_{13}$; ^{19}F NMR ($CDCl_3$): δ −81.5 (3F, s, *a*), −126.2 (2F, s, *b*), −123.4 (2F, s, *c*), −122.3 (2F, s, *d*), −122.0 (2F, s, *e*), −111.4 (2F, s, *f*) for $CF_3{}^aCF_2{}^bCF_2{}^cCF_2{}^dCF_2{}^eCF_2{}^fC_6H_4CH(OH)C_5H_{11}$; GC–MS 70 eV, *m/z* (rel. int.): 496 $[M]^+$ (0.66), 425 $[M–C_5H_{11}]^+$ (100), 377 $[C_6F_{12}C_6H_5]^+$ (19), 156 $[CF_2C_6H_4CH(OH)]^+$ (15), 127 $[CF_2C_6H_5]^+$ (24).

F8PH5A: white solid; IR (cm^{-1}): 3124–3560 ($\nu_{O–H}$), 2816–3000 ($\nu_{C–H}$), 1240 ($\nu_{C–F}$); ^1H NMR ($CDCl_3$): δ 0.88 (3H, t, $J = 7.4$ Hz, *a*), 1.30 (6H, m, *b*, *c* and *d*), 1.73 (2H, m, *e*), 4.73 (1H, t, $J = 5.7$ Hz, *f*), 1.93 (1H, s, *g*), 7.49 (2H, d, $J = 8.1$ Hz, *m*-protons from C_8F_{17}), 7.55 (2H, d, $J = 8.2$ Hz, *o*-protons from C_8F_{17}) for $CH_3{}^aCH_2{}^bCH_2{}^cCH_2{}^dCH_2{}^eCH^f(OH)^gC_6H_4C_8F_{17}$; ^{19}F NMR ($CDCl_3$): δ −81.3 (3F, s, *a*), −126.6 (2F, s, *b*), −123.3 (2F, s, *c*), −122.3 (6F, s, *d*, *e* and *f*), −121.7 (2F, s, *g*), −111.4 (2F, s, *h*) for $CF_3{}^aCF_2{}^bCF_2{}^cCF_2{}^dCF_2{}^eCF_2{}^fCF_2{}^gCF_2{}^hC_6H_4CH(OH)C_5$-$H_{11}$; GC–MS 70 eV, *m/z* (rel. int.): 596 $[M]^+$ (0.41), 525 $[M–C_5H_{11}]^+$ (100), 477 $[C_8F_{16}C_6H_5]^+$ (8.5), 156 $[CF_2C_6$-$H_4CH(OH)]^+$ (6.1), 127 $[CF_2C_6H_5]^+$ (11).

F4PH7A: colorless liquid; IR (cm^{-1}): 3125–3561 ($\nu_{O–H}$), 2816–3002 ($\nu_{C–H}$), 1235 ($\nu_{C–F}$); ^1H NMR ($CDCl_3$): δ 0.87 (3H, t, $J = 5.8$ Hz, *a*), 1.20 (10H, m, *b*, *c*, *d*, *e* and *f*), 1.71 (2H, m, *g*), 4.76 (1H, t, $J = 5.8$ Hz, *h*), 2.03 (1H, s, *i*), 7.46 (2H, d, $J = 8.1$ Hz, *m*-protons from C_4F_9), 7.56 (2H, d, $J = 8.2$ Hz, *o*-protons from C_4F_9) for $CH_3{}^aCH_2{}^bCH_2{}^cCH_2{}^d$-$CH_2{}^eCH_2{}^fCH_2{}^gCH^h(OH)^iC_6H_4C_4F_9$; ^{19}F NMR ($CDCl_3$): δ −81.3 (3F, s, *a*), −126.6 (2F, s, *b*), −122.3 (2F, s, *c*), −111.2 (2F, s, *d*) for $CF_3{}^aCF_2{}^bCF_2{}^cCF_2{}^dC_6H_4CH(OH)C_7H_{15}$; GC–MS 70 eV, *m/z* (rel. int.): 424 $[M]^+$ (1.2), 325 $[M–C_7H_{15}]^+$ (100), 277 $[C_4F_8C_6H_5]^+$ (33), 156 $[CF_2C_6H_4CH(OH)]^+$ (5.4), 127 $[CF_2C_6H_5]^+$ (23).

F6PH7A: white solid; IR (cm^{-1}): 3136–3565 ($\nu_{O–H}$), 2816–3024 ($\nu_{C–H}$), 1245 ($\nu_{C–F}$); ^1H NMR ($CDCl_3$): δ 0.80 (3H, t, $J = 6.6$ Hz, *a*), 1.20 (10H, m, *b*, *c*, *d*, *e* and *f*), 1.65 (2H, m, *g*), 4.67 (1H, t, $J = 5.9$ Hz, *h*), 1.86 (1H, s, *i*), 7.40 (2H, d, $J = 8.1$ Hz, *m*-protons from C_6F_{13}), 7.49 (2H, d, $J = 8.2$ Hz, *o*-protons from C_6F_{13}) for $CH_3{}^aCH_2{}^bCH_2{}^cCH_2{}^dCH_2{}^eCH_2{}^fCH_2{}^gCH^h(OH)^iC_6H_4C_6F_{13}$; ^{19}F NMR ($CDCl_3$): δ −81.5 (3F, s, *a*), −126.2 (2F, s, *b*), −123.4 (2F, s, *c*), −122.3 (2F, s, *d*), −122.0 (2F, s, *e*), −111.0 (2F, s, *f*) for $CF_3{}^aCF_2{}^bCF_2{}^cCF_2{}^dCF_2{}^eCF_2{}^fC_6H_4$-$CH(OH)C_7H_{15}$; GC–MS 70 eV, *m/z* (rel. int.): 524 $[M]^+$ (1.4), 425 $[M–C_7H_{15}]^+$ (100), 377 $[C_4F_8C_6H_5]^+$ (35), 156 $[CF_2C_6H_4CH(OH)]^+$ (6.7), 127 $[CF_2C_6H_5]^+$ (25).

F8PH7A: white solid; IR (cm^{-1}): 3124–3560 ($\nu_{O–H}$), 2826–2995 ($\nu_{C–H}$), 1240 ($\nu_{C–F}$); ^1H NMR ($CDCl_3$): δ 0.85 (3H, t, $J = 6.6$ Hz, *a*), 1.29 (10H, m, *b*, *c*, *d*, *e* and *f*), 1.75 (2H, m, *g*), 4.75 (1H, t, $J = 5.8$ Hz, *h*), 1.95 (1H, s, *i*), 7.47 (2H, d, $J = 8.1$ Hz, *m*-protons from C_8F_{17}), 7.56 (2H, d, $J = 8.2$ Hz, *o*-protons from C_8F_{17}) for $CH_3{}^aCH_2{}^bCH_2{}^cCH_2{}^dCH_2{}^eCH_2{}^fCH_2{}^gCH^h(OH)^iC_6H_4C_8F_{17}$; ^{19}F NMR ($CDCl_3$): δ −81.3 (3F, s, *a*), −126.6 (2F, s, *b*), −123.3 (2F, s, *c*), −122.3 (6F, s, *d*, *e* and *f*), −121.7 (2F, s, *g*), −111.3 (2F, s, *h*) for $CF_3{}^aCF_2{}^bCF_2{}^cCF_2{}^dCF_2{}^eCF_2{}^fCF_2{}^g$-$CF_2{}^hC_6H_4CH(OH)C_7H_{15}$; GC–MS 70 eV, *m/z* (rel. int.): 624 $[M]^+$ (0.9), 525 $[M–C_7H_{15}]^+$ (100), 477 $[C_8F_{16}C_6H_5]^+$ (37), 156 $[CF_2C_6H_4CH(OH)]^+$ (10), 127 $[CF_2C_6H_5]^+$ (30).

4.4. Synthesis of hybrid surfactants

4.4.1. Synthesis of sodium 1-[4-(perfluorobutyl)phenyl]-1-butylsulfate (F4PH3OS)

A mixture of F4PH3A (5.00 g, 13.6 mmol), sulfur trioxide/pyridine complex (2.38 g, 15.0 mmol), and pyridine (20 cm^3) were stirred at 50 °C for 24 h. An aqueous solution containing sodium hydroxide (1.2 g, 30.0 mmol) in water (10 cm^3) was added to the reaction mixture and the resultant aqueous mixture was stirred for 10 min. After pyridine and water were removed by distillation under reduced pressure, the methanol-soluble part of the residue was precipitated from hexane to give a white solid as F4PH3OS. Yield 5.31 g (83.0%); IR (cm^{-1}): 2806–3064 ($\nu_{C–H}$), 1225 ($\nu_{C–F}$); ^1H NMR (CD_3OD): δ 0.83 (3H, t, $J = 7.1$ Hz, *a*), 1.39 (2H, m, *b*), 1.73 (2H, dd, *c*), 5.27 (1H, t, $J = 5.7$ Hz, *d*), 7.51 (4H, s, *e*) for $CH_3{}^aCH_2{}^bCH_2{}^cCH^d(OSO_3Na)C_6H_4{}^eC_4F_9$; ^{19}F NMR (CD_3OD): δ −81.3 (3F, s, *a*), −127.3 (2F, s, *b*), −122.7 (2F, s, *c*), −111.2 (2F, s, *d*) for $CF_3{}^aCF_2{}^bCF_2{}^cCF_2{}^dC_6H_4$-$CH(OSO_3Na)C_3H_7$; FABMS *m/z* (rel. int.): 917 $[2M–Na]^-$ (8.8), 447 $[M–Na]^-$ (100), 97 $[OSO_3H]^-$ (19), 80 $[SO_3]^-$ (15).

4.4.2. Synthesis of sodium 1-[4-(perfluorohexyl)phenyl]-1-butylsulfate (F6PH3OS), etc.

The methods of synthesis and purification were the same as those in Section 4.4.1.

F6PH3OS: white solid; yield 79.0%; IR (cm^{-1}): 2812–3065 ($\nu_{C–H}$), 1227 ($\nu_{C–F}$); ^1H NMR (CD_3OD): δ 0.92 (3H, t, $J = 8.0$ Hz, *a*), 1.39 (2H, m, *b*), 1.83 (2H, dd, *c*), 5.33 (1H, t,

$J = 4.7$ Hz, *d*), 7.59 (4H, s, *e*) for $CH_3{}^aCH_2{}^bCH_2{}^cCH^d$-$(OSO_3Na)C_6H_4{}^eC_6F_{13}$; ^{19}F NMR (CD_3OD): δ −82.3 (3F, s, *a*), −127.1 (2F, s, *b*), −123.7 (2F, s, *c*), −122.7 (2F, s, *d*), −122.2 (2F, s, *e*), −111.2 (2F, s, *f*) for $CF_3{}^aCF_2{}^bCF_2{}^cCF_2{}^d$-$CF_2{}^eCF_2{}^fC_6H_4CH(OSO_3Na)C_3H_7$; FABMS *m*/*z* (rel. int.): 1117 $[2M–Na]^-$ (10), 547 $[M–Na]^-$ (100), 97 $[OSO_3H]^-$ (6.2), 80 $[SO_3]^-$ (6.2).

F8PH3OS: white solid; yield 88.3%; IR (cm^{-1}): 2806–3064 ($\nu_{C–H}$), 1225 ($\nu_{C–F}$); ^1H NMR (CD_3OD): δ 0.84 (3H, t, $J = 7.3$ Hz, *a*), 1.32 (2H, m, *b*), 1.69 (2H, dd, *c*), 5.27 (1H, t, $J = 5.5$ Hz, *d*), 7.45 (4H, s, *e*) for $CH_3{}^aCH_2{}^bCH_2{}^cCH^d$-$(OSO_3Na)C_6H_4{}^eC_8F_{17}$; ^{19}F NMR (CD_3OD): δ −82.1 (3F, s, *a*), −127.3 (2F, s, *b*), −123.5 (2F, s, *c*), −122.6 (6F, s, *d*, *e* and *f*), −122.2 (2F, s, *g*), −111.2 (2F, s, *h*) for $CF_3{}^aCF_2{}^bCF_2{}^cCF_2{}^dCF_2{}^eCF_2{}^fCF_2{}^gCF_2{}^hC_6H_4CH(OSO_3Na)$-$C_3H_7$; FABMS *m*/*z* (rel. int.): 1317 $[2M–Na]^-$ (16), 647 $[M–Na]^-$ (100), 97 $[OSO_3H]^-$ (13), 80 $[SO_3]^-$ (6.8).

F4PH5OS: white solid; yield 78.8%; IR (cm^{-1}): 2804–3073 ($\nu_{C–H}$), 1228 ($\nu_{C–F}$); ^1H NMR (CD_3OD): δ 0.76 (3H, t, $J = 5.4$ Hz, *a*), 1.22 (6H, m, *b*, *c* and *d*), 1.69 (2H, dd, *e*), 5.25 (1H, t, $J = 6.4$ Hz, *f*), 7.49 (4H, s, *g*) for CH_3-$^aCH_2{}^bCH_2{}^cCH_2{}^dCH_2{}^eCH^f(OSO_3Na)C_6H_4{}^gC_4F_9$; ^{19}F NMR (CD_3OD): δ −82.1 (3F, s, *a*), −127.3 (2F, s, *b*), −122.7 (2F, s, *c*), −111.2 (2F, s, *d*) for $CF_3{}^aCF_2{}^bCF_2{}^cCF_2{}^dC_6H_4$-$CH(OSO_3Na)C_5H_{11}$; FABMS *m*/*z* (rel. int.): 973 $[2M–Na]^-$ (26), 475 $[M–Na]^-$ (100), 97 $[OSO_3H]^-$ (6.2), 80 $[SO_3]^-$ (6.2).

F6PH5OS: white solid; yield 70.4%; IR (cm^{-1}): 2806–3080 ($\nu_{C–H}$), 1230 ($\nu_{C–F}$); ^1H NMR (CD_3OD): δ 0.80 (3H, t, $J = 4.7$ Hz, *a*), 1.18 (6H, m, *b*, *c* and *d*), 1.75 (2H, dd, *e*), 5.28 (1H, t, $J = 6.4$ Hz, *f*), 7.53 (4H, s, *g*) for $CH_3{}^aCH_2{}^bCH_2{}^cCH_2{}^dCH_2{}^eCH^f(OSO_3Na)C_6H_4{}^gC_6F_{13}$; ^{19}F NMR (CD_3OD): δ −82.1 (3F, s, *a*), −127.1 (2F, s, *b*), −123.7 (2F, s, *c*), −122.7 (2F, s, *d*), −122.2 (2F, s, *e*), −111.1 (2F, s, *f*) for $CF_3{}^aCF_2{}^bCF_2{}^cCF_2{}^dCF_2{}^eCF_2{}^fC_6H_4$-$CH(OSO_3Na)C_5H_{11}$; FABMS *m*/*z* (rel. int.): 1173 $[2M–Na]^-$ (1.0), 575 $[M–Na]^-$ (100), 97 $[OSO_3H]^-$ (4.9), 80 $[SO_3]^-$ (4.9).

F8PH5OS: white solid; yield 75.4%; IR (cm^{-1}): 2810–3070 ($\nu_{C–H}$), 1227 ($\nu_{C–F}$); ^1H NMR (CD_3OD): δ 0.82 (3H, t, $J = 5.4$ Hz, *a*), 1.20 (6H, m, *b*, *c* and *d*), 1.69 (2H, dd, *e*), 5.26 (1H, t, $J = 6.1$ Hz, *f*), 7.56 (4H, s, *g*) for $CH_3{}^aCH_2{}^bCH_2{}^cCH_2{}^dCH_2{}^eCH^f(OSO_3Na)C_6H_4{}^gC_8F_{17}$; ^{19}F NMR (CD_3OD): δ −82.1 (3F, s, *a*), −127.1 (2F, s, *b*), −123.5 (2F, s, *c*), −122.7 (6F, s, *d*, *e* and *f*), −122.2 (2F, s, *g*), −111.2 (2F, s, *h*) for $CF_3{}^aCF_2{}^bCF_2{}^cCF_2{}^dCF_2{}^eCF_2{}^fCF_2{}^g$-$CF_2{}^hC_6H_4CH(OSO_3Na)C_5H_{11}$; FABMS *m*/*z* (rel. int.): 1373 $[2M–Na]^-$ (16), 675 $[M–Na]^-$ (100), 97 $[OSO_3H]^-$ (19), 80 $[SO_3]^-$ (13).

F4PH7OS: white solid; yield 69.3%; IR (cm^{-1}): 2812–3067 ($\nu_{C–H}$), 1230 ($\nu_{C–F}$); ^1H NMR (CD_3OD): δ 0.77 (3H, t, $J = 4.2$ Hz, *a*), 1.16 (10H, m, *b*, *c*, *d*, *e* and *f*), 1.71 (2H, dd, *g*), 5.25 (1H, t, $J = 6.4$ Hz, *h*), 7.53 (4H, s, *i*) for $CH_3{}^aCH_2{}^bCH_2{}^cCH_2{}^dCH_2{}^eCH_2{}^fCH_2{}^gCH^h$ (OSO_3Na)-$C_6H_4{}^iC_4F_9$; ^{19}F NMR (CD_3OD): δ −82.2 (3F, s, *a*), −127.3 (2F, s, *b*), −122.6 (2F, s, *c*), −111.2 (2F, s, *d*) for $CF_3{}^aCF_2{}^bCF_2{}^cCF_2{}^dC_6H_4CH(OSO_3Na)C_7H_{15}$; FABMS *m*/*z* (rel. int.): 1029 $[2M–Na]^-$ (10), 503 $[M–Na]^-$ (100), 97 $[OSO_3H]^-$ (20), 80 $[SO_3]^-$ (15).

F6PH7OS: white solid; yield 70.4%; IR (cm^{-1}): 2811–3090 ($\nu_{C–H}$), 1245 ($\nu_{C–F}$); ^1H NMR (CD_3OD): δ 0.64 (3H, t, $J = 4.6$ Hz, *a*), 1.18 (10H, m, *b*, *c*, *d*, *e* and *f*), 1.60 (2H, dd, *g*), 5.26 (1H, t, $J = 6.4$ Hz, *h*), 7.49 (4H, s, *i*) for $CH_3{}^aCH_2{}^bCH_2{}^cCH_2{}^dCH_2{}^eCH_2{}^fCH_2{}^gCH^h$ (OSO_3Na)-$C_6H_4{}^iC_6F_{13}$; ^{19}F NMR (CD_3OD): δ −82.1 (3F, s, *a*), −127.1 (2F, s, *b*), −123.7 (2F, s, *c*), −122.7 (2F, s, *d*), −122.2 (2F, s, *e*), −111.1 (2F, s, *f*) for $CF_3{}^aCF_2{}^bCF_2{}^cCF_2{}^d$-$CF_2{}^eCF_2{}^fC_6H_4CH(OSO_3Na)C_7H_{15}$; FABMS *m*/*z* (rel. int.): 1429 $[2M–Na]^-$ (11), 703 $[M–Na]^-$ (100), 97 $[OSO_3H]^-$ (25), 80 $[SO_3]^-$ (20).

F8PH7OS: white solid; yield 69.3%; IR (cm^{-1}): 2812–3067 ($\nu_{C–H}$), 1230 ($\nu_{C–F}$); ^1H NMR (CD_3OD): δ 0.77 (3H, t, $J = 4.2$ Hz, *a*), 1.16 (10H, m, *b*, *c*, *d*, *e* and *f*), 1.71 (2H, dd, *g*), 5.25 (1H, t, $J = 6.4$ Hz, *h*), 7.53 (4H, s, *i*) for $CH_3{}^aCH_2{}^bCH_2{}^cCH_2{}^dCH_2{}^eCH_2{}^fCH_2{}^gCH^h(OSO_3Na)C_6H_4{}^i$-$C_8F_{17}$; ^{19}F NMR (CD_3OD): δ −82.2 (3F, s, *a*), −127.3 (2F, s, *b*), −123.5 (2F, s, *c*), −122.6 (6F, s, *d*, *e* and *f*), −122.2 (2F, s, *g*), −111.2 (2F, s, *h*) for $CF_3{}^aCF_2{}^bCF_2{}^cCF_2{}^dCF_2{}^eCF_2{}^fCF_2{}^g$-$CF_2{}^hC_6H_4CH(OSO_3Na)C_7H_{15}$; FABMS *m*/*z* (rel. int.): 1029 $[2M–Na]^-$ (10), 503 $[M–Na]^-$ (100), 97 $[OSO_3H]^-$ (20), 80 $[SO_3]^-$ (15).

References

[1] H.G. Bryce, in: J.H. Simons (Ed.), Fluorine Chemistry, vol. 5, Academic Press, New York, 1950, p. 370.
[2] H. Liebig, K. Ulm, Chem. Zeit. 100 (1976) 3–14.
[3] E. Schuierer, Tenside 13 (1976) 1–5.
[4] K. Shinoda, M. Hato, T. Hayashi, J. Phys. Chem. 76 (1972) 909–914.
[5] Y. Muto, K. Esumi, K. Meguro, R. Zana, J. Colloid Interface Sci. 120 (1987) 162–171.
[6] S.J. Burkitt, B.T. Ingram, R.H. Ottewill, Prog. Colloid Polym. Sci. 76 (1988) 247–250.
[7] K. Kalyanasundaram, Langmuir 4 (1988) 942–945.
[8] H. Matsuki, N. Ikeda, M. Aratono, S. Kaneshina, K. Motomura, J. Colloid Interface Sci. 150 (1992) 331–337.
[9] M. Abe, T. Yamaguchi, Y. Shibata, H. Uchiyama, K. Ogino, N. Yoshino, S.D. Christian, Colloids Surf. 67 (1992) 29–35.
[10] K. Kamogawa, K. Tajima, J. Phys. Chem. 97 (1993) 9506–9512.
[11] W. Guo, Z. Li, B.M. Fung, E.A. O'Rear, J.H. Harwell, J. Phys. Chem. 96 (1992) 6738–6742.
[12] N. Yoshino, K. Hamano, Y. Omiya, Y. Kondo, A. Ito, M. Abe, Langmuir 11 (1995) 466–469.
[13] M. Abe, K. Tobita, H. Sakai, Y. Kondo, N. Yoshino, Y. Kasahara, H. Matsuzawa, M. Iwahashi, N. Momozawa, K. Nishiyama, Langmuir 13 (1997) 2932–2934.
[14] K. Tobita, H. Sakai, Y. Kondo, N. Yoshino, M. Iwahashi, N. Momozawa, M. Abe, Langmuir 13 (1997) 5054–5055.
[15] K. Tobita, H. Sakai, Y. Kondo, N. Yoshino, K. Kamogawa, N. Momozawa, M. Abe, Langmuir 14 (1998) 4753–4757.
[16] M. Abe, K. Tobita, H. Sakai, K. Kamogawa, N. Momozawa, Y. Kondo, N. Yoshino, Colloids Surf. A Physicochem. Eng. Aspects 167 (2000) 47–60.
[17] M. Abe, N. Yoshino, J. Jpn. Oil. Chem. 45 (1996) 991–999.
[18] M. Abe, A. Saeki, K. Kamogawa, H. Sakai, Y. Kondo, N. Yoshino, H. Uchiyama, J.H. Harwell, Ind. Eng. Chem. Res. 39 (2000) 2697–2703.

[19] A. Ito, H. Sakai, Y. Kondo, N. Yoshino, M. Abe, Langmuir 12 (1996) 5768–5772.
[20] M.J. Rosen, Surfactants and Interfacial Phenomena, second ed., Wiley, New York, 1989 (Chapters 2 and 3).
[21] Y. Kondo, H. Miyazawa, H. Sakai, M. Abe, N. Yoshino, J. Am. Chem. Soc. 124 (2002) 6516–6517.
[22] N. Muller, E.F. Platko, J. Phys. Chem. 75 (1971) 547–553.
[23] B.-O. Persson, T. Drakenberg, B. Lindman, J. Phys. Chem. 83 (1979) 3011–3015.
[24] S. Braun, H.-O. Kalinowski, S. Berger, 150 and More Basic NMR Experiments, Wiley-VCH, Weinheim, 1998, p. 442.
[25] M. Holz, H. Weingärtner, J. Magn. Reson. 92 (1991) 115–125.